Search a new core materials for magnetic fluid hyperthermia : preliminary chemical and physical issues

Emil Pollert, Pavel Veverka, Miroslav Veverka, Ondřej Kaman, Karel Závěta, Sébastien Vasseur, Romain Epherre, Graziella Goglio, Etienne Duguet

Search of New Core Materials for Magnetic Fluid Hyperthermia: Preliminary Chemical and Physical Issues

E. Pollert[1*], P. Veverka[1], M. Veverka[1], O. Kaman[1,2], K. Závěta[1,3], S. Vasseur[4], R. Epherre[4], G. Goglio[4], E. Duguet[4]

[1] Institute of Physics, ASCR, Cukrovarnická 10, 16253 Praha 6, Czech Republic

[2] Faculty of Sciences, Charles University, Albertov 6, 12843 Praha 2, Czech Republic

[3] Joint Laboratory of Mossbauer Spectroscopy, Faculty of Mathematics and Physics, Charles University, 18000 Praha 8, Czech Republic

[4] CNRS, Université de Bordeaux, Institut de Chimie de la Matière Condensée de Bordeaux, 87 avenue du Dr Albert Schweitzer, 33608 Pessac, France

Abstract

Today the use of nanoparticles based on magnetite Fe_3O_4 or maghemite γ-Fe_2O_3 for magnetic fluid hyperthermia (MFH) application is preferred for evident reasons as biocompatibility and easy synthesis. However, they only show moderate heating capacities because their magnetic properties cannot be simply adjusted to a suitable level. A possible improvement of the MFH technique consists in using more complex magnetic oxides such as: (i) cobalt ferrite and derived phases whose magnetic properties depend on the composition and coercivity is essentially controlled by the magnetocrystalline and/or shape anisotropy, (ii) $La_{1-x}Sr_xMnO_3$ perovskites whose magnetic properties are influenced by the composition and crystallite size, (iii) $SrFe_{12}O_{19}$/γ-Fe_2O_3 composites whose magnetic properties are mainly controlled by the ratio of the respective magnetic phases. Our main results concerning the synthesis of these compounds in the form of submicronic particles, their magnetic properties and their heating abilities are summarized, compared and discussed in this paper.

Introduction

Among various therapeutic methods in oncology, there is a continuous increase of an interest for the magnetic fluid hyperthermia (MFH) mostly as a complementary route to chemotherapy and radiotherapy [1 - 6]. The concept of hyperthermia is based on the higher heat-sensitivity of tumour cells. So, treating tumour regions at temperatures between 42 and 45 °C would allow to destroy tumour cells and to spare

* Corresponding author, Fax: +420 233 343 184, E-mail: pollert@fzu.cz

the healthy ones. MFH is a promising hyperthermia modality taking advantage from the capacity of magnetic nanoparticles to convert into heat the energy absorbed from a high-frequency magnetic field mostly via magnetic losses. The clinical protocol would consist in the administration of stable and non-toxic suspensions of the magnetic nanoparticles followed by a short-time exposure to the AC magnetic field. The magnetic fluids that are currently developed are made of inorganic magnetic cores that are (i) simply stabilized by electrostatic repulsions in the case of a direct injection into the tumour [1] or (ii) preferentially embedded in a hydrophilic macromolecular corona for improving their blood half time in the case of intravenous administration [2].

Neglecting frictional losses, two loss mechanisms and consequently two kinds of magnetic cores are generally distinguished. In superparamagnetic particles, loss mechanism results from the rotation of magnetic moments in overcoming the energy barrier $E = KV$, where K is the anisotropy constant and V is the volume of the magnetic core. Energy is dissipated when the particle moment relaxes to its equilibrium orientation; this phenomenon is known as Néel relaxation. In ferro- or ferrimagnetic particles, heating is due to hysteresis losses [7, 8]. Successful use of the latter type requires the maintenance of the magnitude of magnetization for small particles as high as possible. Further the coercivity should be adjusted to a reasonable value assuring sufficient heating efficiency, but not too high with respect to technical restrictions on the field amplitude for practical medical heating application, i.e. about $8 – 16\ kA \cdot m^{-1}$. At the same time, attention should be paid to the applied frequency. It has to be higher than 50 kHz to avoid neuromuscular electrostimulation and lower than 10 MHz, rather below 2 MHz, in order to achieve a reasonable penetration depth of the rf-field. Therefore it is obvious that an improvement cannot be achieved only by modulation of the parameters of the applied AC magnetic field, but also by finely controlling some parameters of the particles such as chemical composition, particle size, size distribution and tune in this manner magnetic properties of the materials.

Until the last decade, magnetite Fe_3O_4 and maghemite γ-Fe_2O_3 were preferred for the MFH development because of their inherent biocompatibility, their easy synthesis in the form of stable aqueous magnetic fluids and their parallel development as contrast agents in magnetic resonance imaging [9]. That is why the majority of *in vitro* and *in vivo* experiments on animals (and very recently on humans) are running with heat mediators based on magnetite or maghemite cores [1]. Their use is, however, associated with some inconveniencies connected with a limited possibility to control

magnetic properties in a desired way. First, they exhibit only medium heating efficiency, characterized by specific absorption rate (SAR), expressed in $W \cdot g^{-1}$ of magnetic element. This factor is, however, crucial for clinical purposes because the higher the value, the lower the needed dose injected to the patient. The second important restriction concerns the control of *in vivo* temperature evolution during hyperthermia, because on one hand the heat conduction and energy adsorption *in vivo* are widely unknown and on the other hand local overheating may damage healthy tissue. An original route could exploit the temperature dependence of magnetic properties. Curie temperature T_c is the temperature above that the ferromagnetic materials lose their strongly magnetic properties and become paramagnetic. So, by designing magnetic nanoparticles with a T_c just above the therapeutic temperature (45 °C, i.e. 318 K), the heating would spontaneously stop as soon as the environment temperature reaches T_c. So, the nanoparticles would act not only as heat mediators but also as *in vivo* temperature control switches [1]. It is obvious that these conditions can be hardly fulfilled by the currently used simple iron oxides, magnetite and maghemite.

A possible approach to solve this task is the use of complex magnetic oxides, whose magnetic properties can be properly tailored by various ways, like (i) the modification of intrinsic properties depending on the composition and structure, or (ii) the modification of extrinsic properties like particle size depending on the synthesis procedure and alternatively employing multiphase materials.

In fact these approaches are usually combined and we have investigated the outlined possibilities on the following three types of magnetic oxides and their systems exhibiting typical distinct features:

Ferrimagnetic spinels, cobalt ferrite, $CoFe_2O_4$ and derived phases

It possesses mixed, spinel structure of the formula $(Co_xFe_{1-x})_A[Co_{1-x}Fe_{1+x}]_BO_4$ where A and B indicate tetrahedral and octahedral sites, respectively. The site occupancy varies from x = 0.20 to 0.07 for rapidly quenched and slowly cooled samples, respectively, from 1200 °C [10]. One can thus suppose that $CoFe_2O_4$ nanoparticles prepared at substantially lower temperatures may have even more complete inverse structure. The bulk $CoFe_2O_4$ is characterized by Curie temperature of $T_c \sim 517$ °C (790 K), saturated magnetization of $M_s \sim 95$ $A \cdot m^2 \cdot kg^{-1}$ and a high magnetocrystalline anisotropy constant of $K_1 = 270 \cdot 10^3$ $J \cdot m^{-3}$ at 20 °C, i.e. 293 K decreasing to $K_1 = 90 \cdot 10^3$ $J \cdot m^{-3}$ at 90 °C, i.e. 363 K [11, 12].

Its properties can be modified by a suitable compositional variation, *e.g.* by replacing cobalt cations by non-magnetic zinc cations, which prefer the tetrahedral sites. The mechanism of the substitution can be described by the general formula $(Zn^{2+}_{x}Fe^{3+}_{(1-x)})_A[Co^{2+}_{(1-x)}Fe^{3+}_{(1+x)}]_BO_4$. At low concentrations of Zn^{2+}, approximately for $0 < x < 0.5$, it leads to an increase of the total moment [13]. But the continuing decrease of the concentration of magnetic ions in the tetrahedral positions ($x > 0.5$) causes a weakening of the A-B interactions and thus leads to a disturbance of the spin ordering causing destabilization of magnetic ordering [14]. An attention should be paid to the influence of the magnetocrystalline anisotropy and shape anisotropy on the coercivity influencing significantly hysteresis losses. As a result the combined influence of the outlined effects can thus offer in a selected range of $0.5 < x < 0.7$ a possibility to tune suitably the magnetic parameters, i.e. Curie temperature, magnetization and coercivity to the values assuring simultaneously a reasonable heating efficiency and the self-controlled heating mechanism in the range of ~ 40 - 60 °C [15 - 17].

Ferromagnetic perovskites $La_{1-x}Sr_xMnO_3$

The parent compound $LaMnO_3$ is a single-valent (Mn^{3+}) antiferromagnetic insulator [18, 19], but replacement of lanthanum by strontium ions causes significant changes of its properties. It leads to a gradual decrease of the steric distortions and structural transition from the orthorhombic (*Pbnm*) to rhombohedral ($R\bar{3}c$) symmetry. Simultaneously by means of the controlled-valence mechanism formally described as $La^{3+}+Mn^{3+} \leftrightarrow Sr^{2+}+Mn^{4+}$, variation of the valencies of manganese ions is induced. Action of both these effects leads to an insulator-metal transition and to ferromagnetic ordering due to double-exchange interactions above $x \sim 0.1$. As it is shown in the magnetic phase diagram established for bulk materials, the Curie temperatures of the ferromagnetic – paramagnetic transition achieve for $0.2 \leq x \leq 0.5$ the values slightly above room temperature namely in the range of 47 – 97 °C, i.e. 320-370 K [20], close to the required condition of the self-controlled heating mechanism.

Therefore attention was paid to a selected composition from this range with $x = 0.25$ possessing the bulk values of T_c = 77 °C, i.e. 350 K and $M_{(1000\ kA\cdot m^{-1})\ 298\ K}$ = 66 $A\cdot m^2\cdot kg^{-1}$. The decrease of crystallite size, typically below ~ 100 nm, leads, however, to a gradual diminution of the stability of the magnetic ordering because of an increasing influence of the outer magnetically "dead layer" [21]. Let us note that alternatively La-Na and La-Ag manganese perovskites, where lanthanum ions are replaced by monovalent sodium or silver, were investigated [22]. They exhibit

analogical properties, i.e. ferromagnetic ordering and Curie temperature below 52 °C i.e. 325 K.

Ferrimagnetic $SrFe_{12}O_{19}/\gamma$-Fe_2O_3 composites

Entirely different approach to solve the outlined task is the use of multiphase materials. Then the combined contribution of considerably magnetically different phases makes it possible to adjust the coercivity, remanence and thus the shape of the hysteresis loop to be appropriate for the magnetic fluid hyperthermia application. A promising possibility thus appears in the use of composite materials consisting of maghemite spinel and Sr-hexaferrite phases employing simultaneously their structural similarity and an important difference of magnetic anisotropies, where $K_1(\gamma\text{-}Fe_2O_3)_{298K} = -25\cdot10^3$ J·m^{-3} [23] and $K_1(SrFe_{12}O_{19})_{298K} = 380\cdot10^3$ J·m^{-3} [24]. Besides that the family of hexagonal ferrites offers with respect to its structural properties possibilities to modify the resulting magnetic properties in two promising ways [25]:

- by compositional variations conditioned by the existence of several cationic sublattices,
- by the stacking defects, i.e. variation of an intergrowth of the individual blocks S, R and T.

Synthesis routes

The syntheses of the magnetic cores are carried out essentially *via* various wet chemistry methods, like coprecipitation, sol-gel methods, water in oil suspension and hydrolysis of metal alkoxides [26 - 37].

A procedure based on a simple coprecipitation from the basic solution of the corresponding salts preferentially nitrates is sufficient for cobalt and cobalt zinc ferrites. Nevertheless an additional annealing at moderate temperatures in the range of ~ 300 – 800 °C and for a relatively short time of 3 h should be used in order to adjust suitably the crystallite size and consequently the coercivity as a result of an increase of the effective anisotropy, see Table 1 and [38, 39].

The situation becomes, however, more involved for the perovskite phase and $SrFe_{12}O_{19}/\gamma$-Fe_2O_3 composites, because of the presence of heavy cations. Then the formation of the desired phases is conditioned by a thermally enhanced diffusion. The wet chemistry route must be completed by a thermal treatment.

The nanoparticles of manganese perovskite $La_{0.75}Sr_{0.25}MnO_3$ are synthesized *via* sol-gel technique employing citric acid and ethylene glycol, accompanied by a subsequent evaporation of water, drying, calcination and annealing for 3 h at

temperatures in the range of 650 – 900 °C giving rise to crystallites ranging from 25 nm to 120 nm. In spite of the relatively low heating temperatures, there appears a tendency to sintering manifested by the formation of "connecting bridges" between the individual grains, an undesirable effect observed by several authors [32, 34, 40 - 41]. It complicates further encapsulation by shells and further stabilization of suspensions. The aggregates should be thus subjected to mechanical treatment (rolling and milling) in order to separate the individual grains [42].

Synthesis of nanoparticles of $SrFe_{12}O_{19}/\gamma\text{-}Fe_2O_3$ composites is based on a method employing polyvinylalcohol as a stabilizing agent. The obtained sols are transformed into gels, dried and calcinated for 3 h at 400 °C. Final heat treatment carried out at temperatures in the range of 600 – 700 °C requires a strict observance of the annealing conditions documented by the growth of the amount of Sr-hexaferrite M-phase with the annealing temperature and time (Figure 1). Let us note that maghemite spinel phase $\gamma\text{-}Fe_2O_3$ arising during the calcination at 400 °C becomes unstable approximately at 600 °C. Its structural affinity provides an easy insertion of the spinel blocks into the hexagonal ferrite stacked structure. A small part of $\gamma\text{-}Fe_2O_3$ is simultaneously converted to hematite $\alpha\text{-}Fe_2O_3$ [43]. A tendency to an intergrowth can be further supported employing a new method based on partial hydrothermal decomposition of pre-synthesized hexaferrite particles [44].

Magnetic properties

The general tendency to destabilization of the magnetic ordering with decreasing crystallite size is substantially suppressed for cobalt ferrite nanoparticles due to its high magneto-crystalline anisotropy. Therefore only a relatively slight decrease of the bulk values of the saturated magnetization M_s ~ 95 $A \cdot m^2 \cdot kg^{-1}$ and of the Curie temperature T_c = 517 °C, i.e. 790 K, respectively, down to M_s ~ 56 - 58 $A \cdot m^2 \cdot kg^{-1}$ and T_c = 462 °C, i.e. 735 K for nanoparticles of the mean size ~ 15 nm is observed. The critical size for the transition to superparamagnetic state appears to be ~ 5 nm around room temperature [26, 27, 45, 46]. Simultaneously the effective anisotropy of the crystallites contributing to the variation of the coercivity and remanent magnetization with crystallite size plays an important role, as it can be seen from the Figure 2 and the data summarized in Table 1, see also [39].

Substitution of cobalt by zinc ions in the series $(Zn^{2+}_{x}Fe^{3+}_{(1-x)})_A[Co^{2+}_{(1-x)}Fe^{3+}_{(1+x)}]_BO_4$ leads to a gradual destabilization of magnetic ordering manifested for nanoparticles

first of all by a decrease of Curie temperature while there is only a slight lowering of the saturated magnetization, see Table 2 and [47].

By contrast $La_{0.75}Sr_{0.25}MnO_3$ perovskite appears to be a significantly "softer" material. An appreciable dependence of magnetization and Curie temperature on the crystallite size given in Figure 3 manifests itself in a gradual deterioration of the magnetic ordering with decreasing size of the crystallites. Our own data are completed by the values reported for the lowest mean crystallite sizes, i.e. 13 and 17 nm, respectively, from [33]. Likewise the critical size of the ferromagnetic–superparamagnetic transition at room temperature ~10 nm estimated on the basis of a simple 3D model of spherical particles is significantly higher than the critical size for cobalt ferrite [21].

An influence of the phase composition of the composite materials is obvious from Figure 4. It is shown that their properties can be modified in a desirable way by changing the ratio between the respective magnetic phases i.e. magnetically soft spinel ferrite and the magnetically hard hexaferrite. An increasing content of M-phase leads to a significant increase of the coercivity and remanence accompanied by a relatively weak enhancement of the magnetization. The important difference of magnetic anisotropies mentioned above has a decisive role. The effect is so strong that the influence of the crystallite size plays, at least for M-phase particles in the range of d ~ 29 - 49 nm, only a minor role (see inset in Figure 4).

Magnetic heating

The present ferrimagnetic and ferromagnetic nanoparticles possess multidomain character and the prevailing mechanism of heating in RF magnetic field is thus due to hysteresis losses P (in $W \cdot g_y^{-1}$) corresponding to the relation

$$P = 1.26 \cdot 10^{-3} \cdot y^{-1} \cdot \nu \cdot \oint_M H \cdot dM \qquad (1)$$

where y is the weight fraction of magnetic elements, ν frequency (in Hz), H magnetic field (in $A \cdot m^{-1}$) and M magnetization of the measured sample (in $A \cdot m^2 \cdot kg^{-1}$). The heating efficiency can be also characterized by a "direct" calorimetric measurement of SAR defined according to [18] as

$$\mathrm{SAR} = (C/x) \cdot (dT/dt) \qquad (2)$$

where C is the specific heat of the medium in which the particles are suspended (usually roughly equal to the specific heat of water, *i.e.* 4.18 $J \cdot g^{-1}$), dT/dt is the slope of the temperature *vs.* time curve and x is the weight fraction of magnetic elements in

the medium. This approach is experimentally realized by the application of an alternating field on a suspension of magnetic particles in a liquid.

Let us note that the power losses P evaluated from the measurements of hysteresis loops agree only qualitatively with the data obtained by calorimetric measurements. One of the reasons for this difference is the influence of the demagnetization factor that strongly depends on the shape of the measured sample. It decides in this way about the value of the inner field and consequently about the resulting magnetic power losses [42]. The other, probably even more important, difference in these two realizations of the transfer of energy from the alternating field to the magnetic particles and the surrounding medium lies in the thermodynamic conditions of the experiment and measurements: whereas in the direct measurement of hysteresis losses we deal with adiabatic conditions, in the SAR experiment the thermal contact with the surrounding medium is decisive for the behavior of the system. Let us remark that in the real application of MFH the situation may be even more complicated when the particles are placed in a moving medium, e.g. blood flow.

The achieved heating efficiencies depend significantly on the material properties outlined briefly in the introductory part. Therefore a magnitude of magnetization as high as possible is required and coercivity should be kept at a reasonable value allowing an appropriate matching with the applied magnetic field amplitudes. In this context, it is evident that the role played by the magnitude of the effective magnetic anisotropy is decisive. We must have in mind, however, that it is difficult to apply the physical parameters in changed circumstances. In particular the DC magnetic properties apparently suitable for high heating efficiency, as high H_c, need not be pertinent for the application with RF magnetic field. In addition, the choice of the AC field amplitude H_{max} is crucial for the resulting heating power of the magnetic material: if it is much lower than the H_c (measured at the same frequency), the material is not very useful but the heating efficiency dramatically rises when the amplitude comes close to the coercive field or alternatively for a constant amplitude of the RF field the heating power may be abruptly changed when H_c crosses this range of fields due to e.g. its change with temperature.

$CoFe_2O_4$ spinel is a typical example of the influence of extremely high effective magnetic anisotropy consisting of the intrinsic magnetocrystalline anisotropy depending on temperature and possibly of the shape anisotropy, depending on the crystallite shape. Both of these effects contribute simultaneously to the magnitude of H_c and consequently for given amplitude H_{max} to the hysteresis losses and heating

efficiency (Figure 5) [38]. The changes have essentially two reasons: one is the decrease of the constant of magnetocrystalline anisotropy with temperature and the second is the increase of the DC coercivity with crystallite size, see Table 1. A decrease of the Curie temperature evoked by replacing of cobalt for zinc ions allows fulfilling an important and required condition of the self-controlled heating mechanism. Simultaneously the values of saturated magnetization remain still reasonable for MFH application. The measured hysteresis losses listed in Table 2 show for x = 0.65 and 0.6 values well comparable with that of the original cobalt ferrite.

The situation differs for manganese perovskite $La_{0.75}Sr_{0.25}MnO_3$. The observed dependence of the heating efficiency on the size of particles in the range of 30 - 50 nm, see Figure 6, originates from the variation of the magnetization given in the inset of the Figure 6, while there is no significant influence of the changes of coercivity, which remains below 8 $kA \cdot m^{-1}$. The time dependence of heating is characterized by a rapid increase of the temperature followed by its stabilization at the equilibrium temperature T_{max} slightly below T_c (Figure 7).

A combined contribution of the magnetic properties of a selected ratio of Sr-hexaferrite and maghemite spinel phases is employed to adjust appropriately the coercivity and remanence of the composites for MFH application. Therefore in this way the values of H_c = 5.2 $kA \cdot m^{-1}$ and 22.3 $kA \cdot m^{-1}$ measured for composites 1 and 2 allow to reach relatively high heating efficiency for the applied H_{max} in the range of 30.2 - 41.4 $kA \cdot m^{-1}$ and frequency ν = 108 kHz (Figure 8). Simultaneously, the measured temperature *vs.* time dependences of these composites offer an appropriate window giving a chance to adjust the maximum achieved temperature to a desired value where the local overheating risk could be ruled out (Figure 9) [48].

Conclusions

The studied mixed oxides belong to various classes of magnetic materials. Each of them could be used as heat mediator for MFH, even if some issues should be solved before their transfer to practice and clinical development. Therefore, it seems useful to compare their respective features and to point out their specific advantages and drawbacks with respect to MFH requirements.

According to the applied methods and achieved experiences, the synthesis of cobalt-zinc ferrite particles formed directly by alkaline coprecipitation (eventually completed by a gentle annealing) evidently appears the easiest. The thermal treatment

has an advantageous influence on the morphology of the grains possessing nearly regular shape and almost uniform size lying in the range of 10 - 20 nm. The process, however, becomes less convenient for manganese perovskites. The first step based on a sol-gel method leads to the formation of precursors preferentially of an amorphous character while the second step, the thermal treatment crucial for an enhanced diffusion of heavy cations, lanthanum and strontium, is accompanied by a tendency to sintering expressed by the formation of bridges connecting the grains. Rolling and milling can successfully effectuate separation of the individual grains, but this handling unfortunately leads to a morphology reminding crushed stone.

A similar problem exists for $SrFe_{12}O_{19}/\gamma$-Fe_2O_3 composites, where the diffusion of strontium ions forced by the thermal treatment is additionally complicated by an instability of γ-Fe_2O_3 around 600 °C. This final step of the synthesis thus becomes hardly reproducible and the products consisting of two types of grains, namely hexaferrite and maghemite tend to agglomeration.

Unfortunately, all three types of nanoparticles, as they are obtained at the end of the synthesis step, cannot be spontaneously dispersed in pure water in a durable way (spontaneous flocculation occurring in few minutes). Nevertheless, this instability could be overcome at the expense of a stabilization strategy based on electrostatic or steric repulsions. More regrettably, with the exception of $SrFe_{12}O_{19}/\gamma$-Fe_2O_3 composites, these nanoparticles are not biocompatible, because of the presence of toxic heavy metals, which are progressively released in cell culture media. We are currently investigating the possibility of embedding them in a stable silica shell. Preliminary results are encouraging and they will be reported as soon as they are confirmed.

With respect to a search of materials manifesting properties suitable for the magnetic heating, the required optimum behaviour is nearly fulfilled for the ferromagnetic perovskites $La_{1-x}Sr_xMnO_3$. In particular, the studies carried out with $La_{0.75}Sr_{0.25}MnO_3$ particles of a size of 30 - 50 nm showed reasonably high heating efficiency at 37 °C, *i.e.* the body temperature. Simultaneously the self-controlled heating mechanism in the range of ~ 40 – 60 °C is adjustable by the proper modification of the Curie temperature.

Due to the extremely high magnetocrystalline anisotropy the magnetic parameters suitable for heating by hysteresis losses of cobalt ferrite $CoFe_2O_4$ were found already for nanoparticles of a size in the range of 15 - 20 nm. Our preliminary studies, however, showed that the properties of nanoparticles, first of all the undesirably high

Curie temperature (T_c = 520 °C for bulk material), could be lowered below 100 °C by the substitution of non-magnetic ions like zinc for cobalt still keeping the saturated magnetization and consequently hysteresis losses at a reasonable value.

The use of composite materials, consisting of Sr-hexaferrite and maghemite phases, is a quite new concept allowing adjustment of the magnetic behaviour, particularly coercivity and remanence, in order to achieve high heating efficiency and simultaneously to control the heating effect by thermal losses. With respect to the character of hexagonal ferrites family one can expect a number of possibilities to modulate suitably the required properties like Curie temperature and coercivity.

Acknowledgements

This study was performed under support of the Academy of Sciences of the Czech Republic (projects 1QS100100553 and KAN200200651), the Grant Agency of the Academy of Sciences of the Czech Republic (project KJB100100701), the Centre National de la Recherche Scientifique and the European Network of Excellence FAME.

References

[1] Jordan A, Scholz R, Maier-Hauff K, Johanssen M, Wust P, Nadobny J, Schmidt H, Deger S, Loening S, Lanksch W, Felix R. J Magn Magn Mater 2001:225:118.

[2] Duguet E, Mornet S, Vasseur S, Devoisselle JM. Nanomed 2006:1:157.

[3] Falk MH, Issels RD. Int J Hyperthermia 2001:17:1.

[4] Hilger I, Kiessling A, Romanus E, Hiergeist R, Rudolf HT, Andrä W, Roskos M, Linss W, Weber P, Weitshies W, Kaiser WA. Nanotech 2004:15:1027.

[5] Hilger I, Hergt R, Kaiser WA. J Magn Magn Mater 2005:293:314.

[6] Mornet S, Vasseur S, Grasset F, Veverka P, Goglio G, Demorgues A, Portier J, Pollert E, Duguet E. Prog Solid State Chemistry 2006:34:237.

[7] Hergt R, Hiergeist R, Hilger I, Kaiser WA. In: Recent Research Developments in Materials Science, Transworld Research Network, 2002.

[8] Andrä W. In: Magnetism in medicine, Wiley-VCH editors. Edited by Andrä W, Nowak H, Eds. 1998. p. 455.

[9] Corot C, Robert P, Idée JM, Port M. Adv Drug Delivery Rev 2006:58:1471.

[10] Sawatzky GA, van der Moude F, Morish AK. J Appl Phys 1968:39:1204.

[11] Bloembergen N. Proc Inst Radio Eng 1956:44:1259.

[12] Tannenwald PE. Phys Rev 1955:99:463.

[13] Duong GV, Turtelli RS, Nunes WC, Schafler E, Hanh N, Grőssinger R, Knobel MJ. Noncrystal Sol 2007:353:805.

[14] Petitt GA, Forester DW. Phys Rev B 1971:4:3912.

[15] Arulmurugan R, Vaidyanathan G, Sendhilnathan S, Jeyadevan BJ. Magn Magn Mater 2006:303:131.

[16] Vaidzanthan G, Sendhilnathan S. Physica B 2008:403:2157.

[17] Gul IH, Abbasi AZ, Amin F, Anis-Ur-Rehman M, Maqsood A. J Magn Magn Mater 2007:311:494.

[18] Brown Jr. WF. Phys Rev 1963:130:1677.

[19] Chikazumi S. Physics of Magnetism. New York: Wiley, 1964 (265 pp).

[20] Asamitsu A, Morimoto Y, Kumai R, Tomioka Y, Tokura Y. Phys Rev B 1996:54:1716.

[21] Vasseur S, Duguet E, Portier J, Goglio G, Mornet S, Hadová E, Knížek K, Maryško M, Veverka P, Pollert E. J Magn Magn Mater 2006:302:315.

[22] Kuznetsov OA, Sorokina ON, Leontiev VG, Shlyakhtin OA, Kovarski AL, Kuznetsov AA. J Magn Magn Mater 2007:311:204.

[23] Shirk BT, Buessem WR. J Appl Phys 1969:40:1294.

[24] Valstyn EP, Hanton JP, Morrish AH. Phys Rev 1962:128:2078.

[25] Pollert E. Crystal chemistry of Magnetic Oxides, Part II. Hexagonal Ferrites. Prog Crystal Growth and Character 1985:11:155.

[26] Kim YI, Kim D, Lee CS. Physica B 2003:337:42.

[27] Carp O, Patron L, Reller A. Mat Chem Phys 2007:101:142.

[28] Moumen N, Veillet P, Pileni MP. J Magn Magn Mater 1995:149:67.

[29] Vaidyanathan G, Sendhilnathan S. Physica B 2008:403:2157.

[30] Uehara M, Takahashi K, Asaka T, Tsutsumi S. J Ceram Soc Jpn 1998:106:1248.

[31] Bae SY, Wang SX. Appl Phys Lett 1996:69:121.

[32] Pang G, Xu X, Markovich V, Avivi S, Palchik O, Koltypin Y, Gorodetsky G, Yeshurun Y, Buchkremer HP, Gedanken A. Mat Res Bull 2003:38:11.

[33] Lipham ND, Tsoi GM, Wenger LE. IEEE Trans Mag 2007:43:3088.

[34] Moreira ML, Soares JM, de Azevedo WM, Rodrigues AR, Machado FLA, de Araújo JH. Physica B 2006:384:51.

[35] Waang HC, Yang Z, Ong CK, Li Y, Wang CS. J Magn Magn Mater 1998:187:129.

[36] Liu X, Wang J, Gan LM, Ng SC, Ding J. J Magn Magn Mater 1998:184:344.

[37] Taketomi S, Ozaki Y, Kawasaki K, Yusa S, Miyajima H. J Magn Magn Mater 1993:122:6.

[38] Lee SW, Bae S, Takemura Y, Shim IB, Tae MK, Kim J, Lee HJ, Zurn S, Kim CS. J Magn Magn Mater 2007:310:2868.

[39] Veverka M, Veverka P, Lančok A, Závěta K, Pollert E, Knížek K, Boháček J, Beneš M, Kašpar P, Duguet E, Vasseur S. Nanotech 2007:18:345704.

[40] Vasseur S, Duguet E, Portier J, Goglio G, Mornet S, Hadová E, Knížek K, Maryško M, Veverka P, Pollert E. J Magn Magn Mater 2006:302:315.

[41] Pang G, Xu X, Markovich V, Avivi S, Palchik O, Koltypin Y, Gorodetsky G, Yeshurun Y, Buchkremer HP, Gedanken A. Mat Res Bull 2003:38:11.

[42] Pollert E, Knížek K, Maryško M, Kašpar P, Vasseur S, Duguet E. J Magn Magn Mater 2007:316:122.

[43] Veverka P, Knížek K, Pollert E, Boháček J, Duguet E, Portier J. J Magn Magn Mater 2007:309:106.

[44] Makovec D, Drofenik M. Crystal Growth & Design 2008:8:2182.

[45] Vandenberghe RE, Vanleerberghe R, de Grave E, Robbrecht G. J Magn Magn Mater 1980:15:1117.

[46] Haneda K, Morrish AH. J Appl Phys 1988:63:4258.

[47] Veverka M, Veverka P, Kaman O, Pollert E, Závěta K. will be published.

[48] Veverka P, Pollert E, Závěta K, Vasseur S, Duguet E. Nanotech 2008:19:215705.

Table 1. Size of crystallites and fundamental magnetic data of the samples A, B and C annealed at 400 °C, 600 °C and 800 °C for 3 hours.

Sample	Annealing temperature [°C]	d_{XRD} [nm]	$M_{800\ kA \cdot m^{-1}}$ [$A \cdot m^2 \cdot kg^{-1}$]	M_r [$A \cdot m^2 \cdot kg^{-1}$]	H_c [$kA \cdot m^{-1}$]
A	400	18	61	14	19
B	600	29	65	25	45
C	800	41	66	26	52

Table 2. Fundamental characteristics and hysteresis losses of $Co_{1-x}Zn_xFe_2O_4$ nanoparticles

x	d_{XRD} [nm]	T_c [K]	M_s (300 K) [$A \cdot m^2 \cdot kg^{-1}$]	P (300 K) [$W \cdot g(Co_{(1-x)}+Fe_2)^{-1}$]
0.55	10	397	53	13.6
0.6	13	365	49	10.95
0.65	13	315	45	0.53

Caption of figures

Figure 1 Influence of the annealing time and temperature on the growth of Sr – hexaferrite M-phase; ■,□ - 600 °C; ●,○ - 650 °C; ▲, △ – 700 °C, formulas of the individual phases are normalized to one-cation composition and [mol% $SrFe_xO_{19}/(1+x)$] + [mol% γ-$Fe_2O_3/2$] + [mol% α-$Fe_2O_3/2$] + [mol% $SrCO_3$] = 100 %, details see in [19].

Figure 2 Evolution of the magnetization of $CoFe_2O_4$ nanoparticles with crystallite size (XRD), T = 300 K, measured in static fields, samples annealed for 3 hours at 400 °C - □, 600 °C - ○ and 800 °C - △.

Figure 3 Dependence of the specific magnetization and Curie temperature on the mean size (XRD) of $La_{0.75}Sr_{0.25}MnO_3$ nanoparticles, ▲, △ data from [33].

Figure 4 Dependence of the remanent magnetization and coercivity on the relative content of the M- hexaferrite phase C_r = mol % ($SrFe_xO_{19}/1+x$)/(mol % ($SrFe_xO_{19}/1+x$) + mol %(γ-$Fe_2O_3/2$)), samples 1, 2, 3, 4 and 5. Dependence of the coercivity on the crystallite size of the M- hexaferrite single phase is shown in the inset.

Figure 5 Field amplitude dependences of SAR (v = 108 kHz), $CoFe_2O_4$ samples - A (d = 18 nm): □ - 42 °C, ■ - 37 °C; B (d = 29 nm): ○ - 42 °C, ● - 37 °C; C (d = 41 nm): △ - 42 °C, × - 37 °C; suspended in agarose gel.

Figure 6 Maximum achieved temperatures and heating efficiencies vs. Curie temperatures of $La_{0.75}Sr_{0.25}MnO_3$ particles suspended in agarose gel, measured at $v \sim 108$ kHz and $H_{max} \sim 110$ $kA \cdot m^{-1}$.

Figure 7 Magnetic heating of $La_{0.75}Sr_{0.25}MnO_3$ particles suspended in agarose gel measured at $v \sim 108$ kHz and $H_{max} \sim 110$ $kA \cdot m^{-1}$.

Figure 8 Field amplitude dependences of SAR (v = 108 kHz) at 37 °C, $SrFe_{12}O_{19}/\gamma$-Fe_2O_3 composites, samples 1, 2, 3, 4, 5, suspended in agarose gel, relative contents of the M-hexaferrite phase C_r see Figure 4.

Figures 9 Magnetic heating of the $SrFe_{12}O_{19}/\gamma$-Fe_2O_3 composites nanoparticles suspended in agarose gel, samples 1, 2, 3, 4, relative contents of the M- hexaferrite phase C_r see Figure 4.

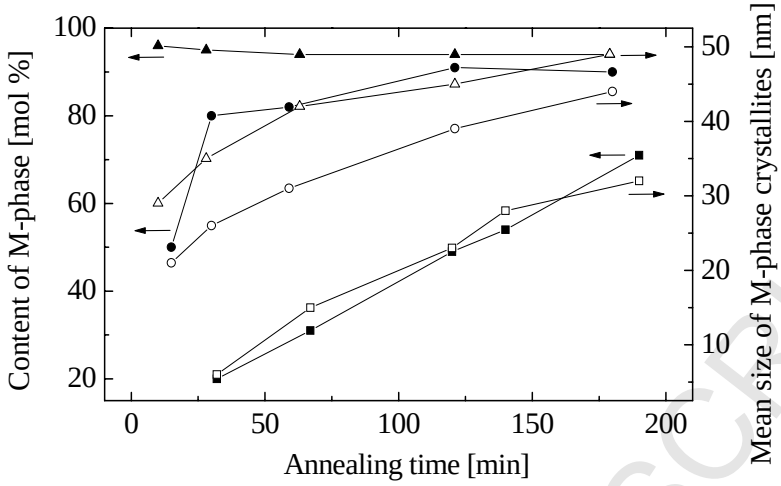

Figure 1

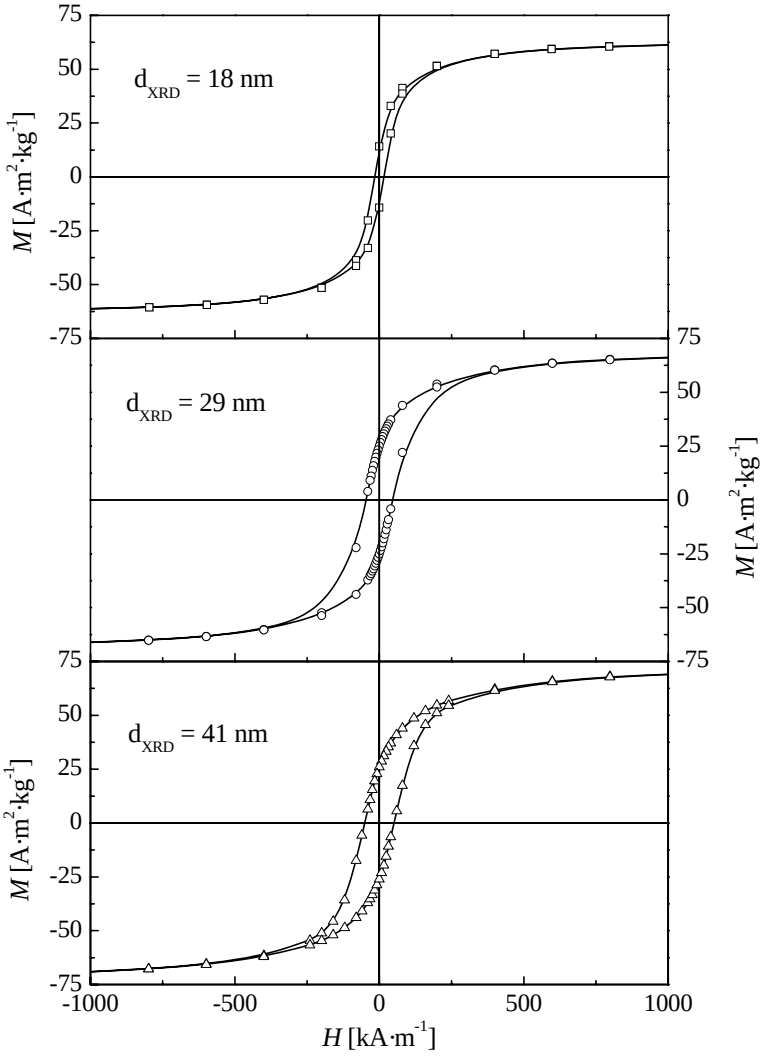
d_XRD = 18 nm
d_XRD = 29 nm
d_XRD = 41 nm
M [A·m²·kg⁻¹]
H [kA·m⁻¹]
75
50
25
0
-25
-50
-75
-1000
-500
0
500
1000

Figure 2

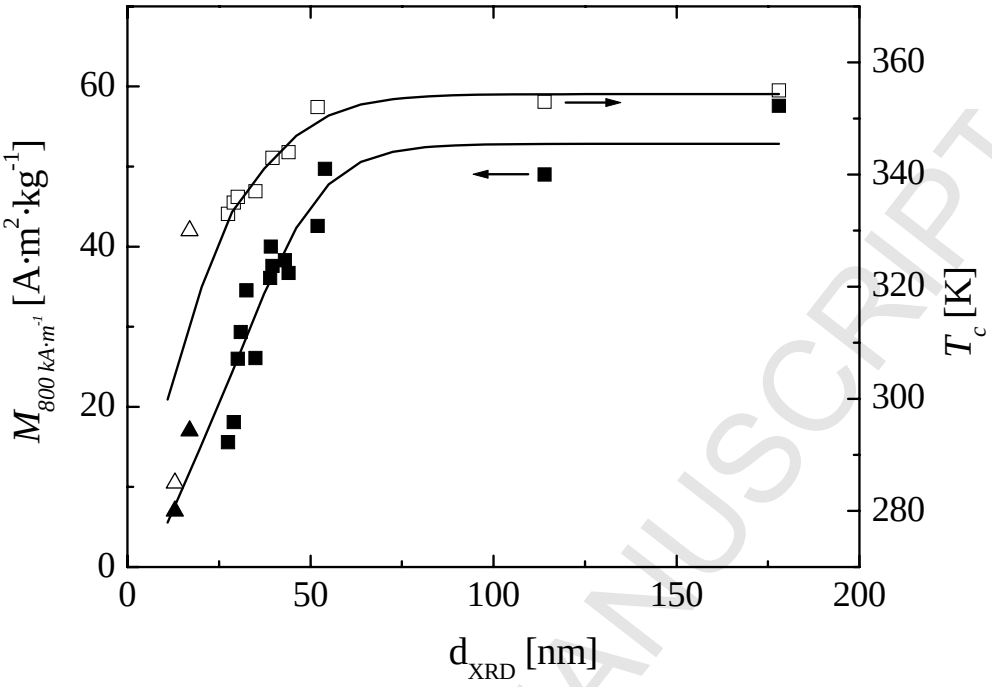

Figure 3

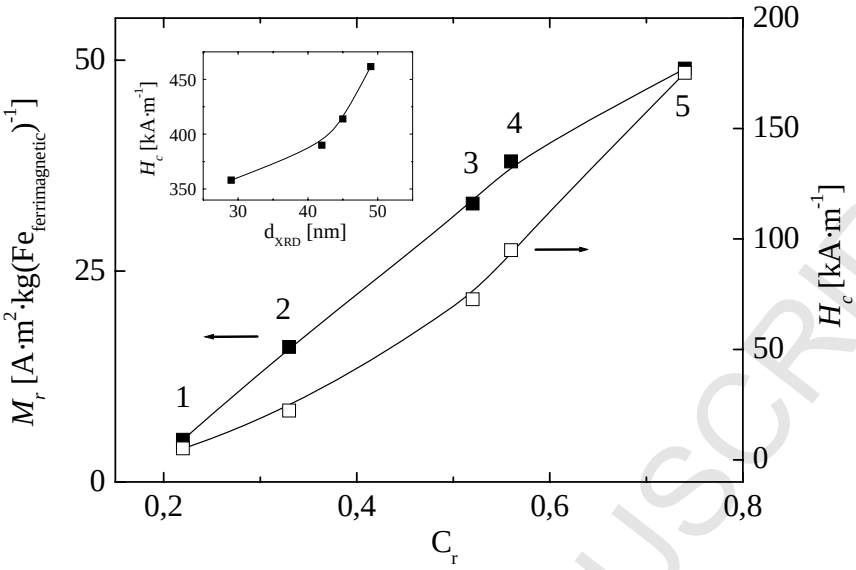

Figure 4

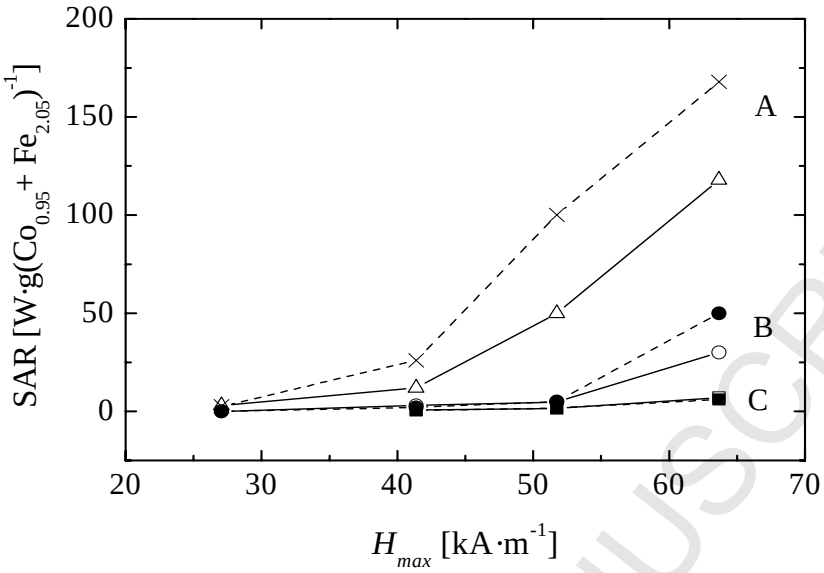

Figure 5

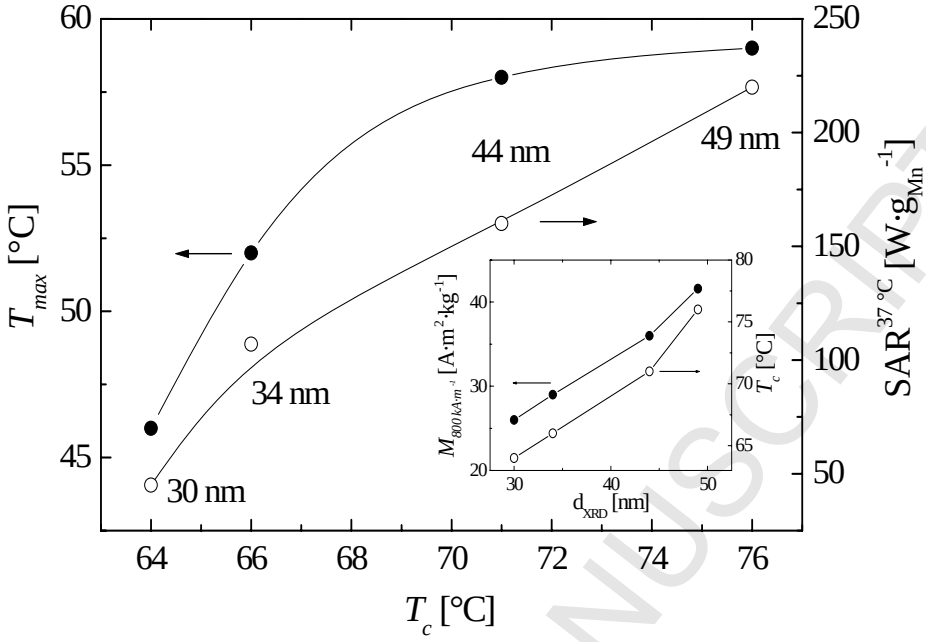

Figure 6

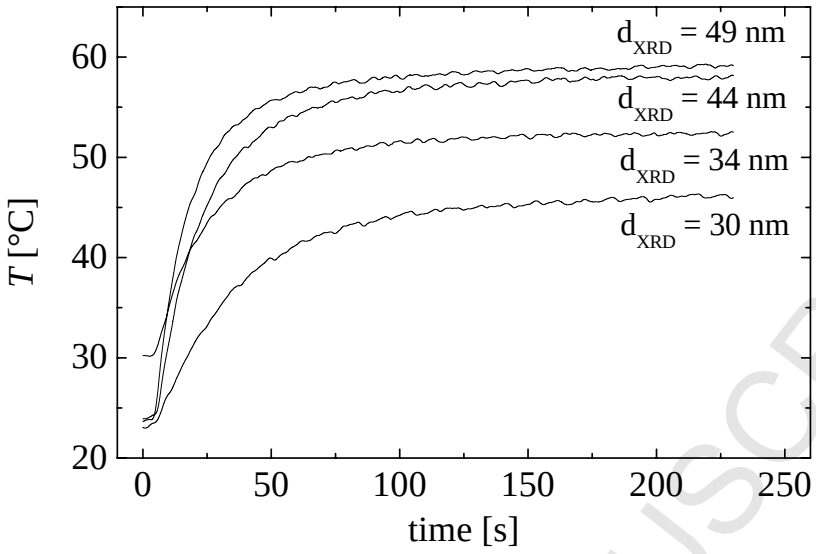

Figure 7

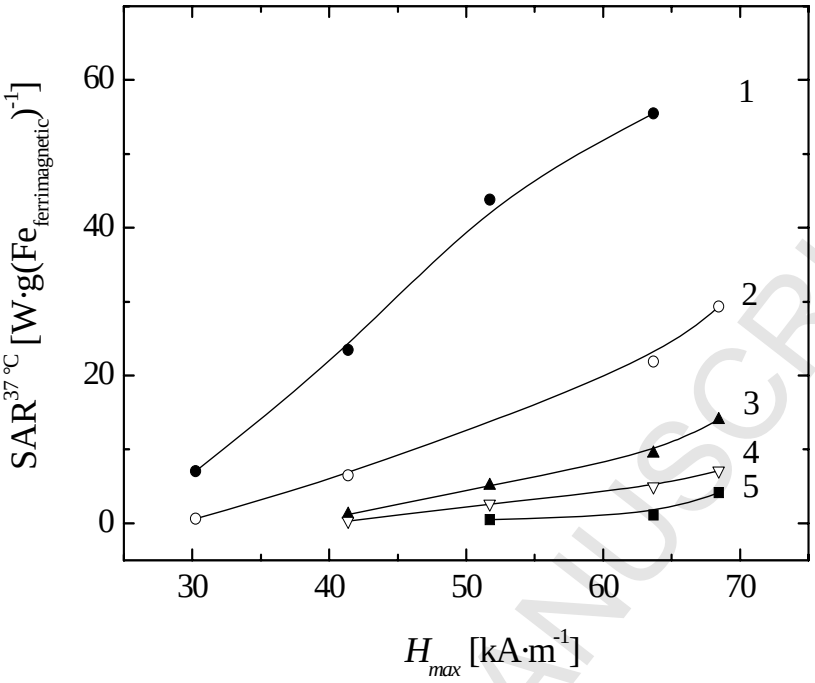

Figure 8

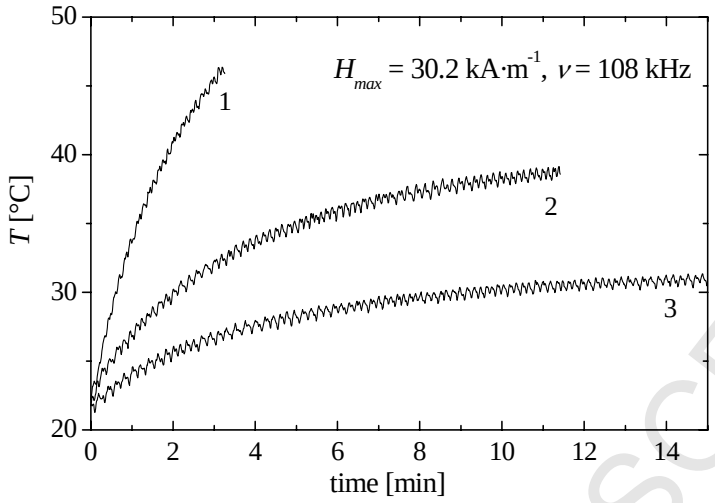

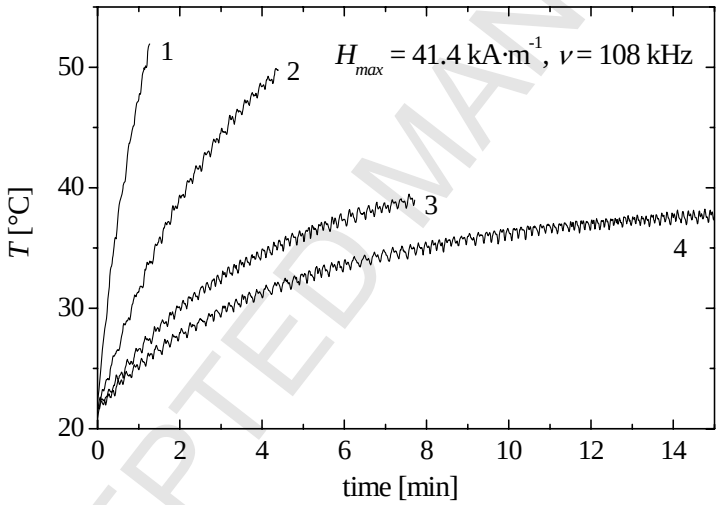

Figures 9